Clin Orthop Relat Res (2009) 467:3213–3220
DOI 10.1007/s11999-009-1087-0

SYMPOSIUM: TRIBUTE TO DR. MARSHALL URIST: MUSCULOSKELETAL GROWTH FACTORS

# Correlation of Computed Tomography with Histology in the Assessment of Periprosthetic Defect Healing

**Stephen D. Cook PhD, Laura P. Patron BSE, Samantha L. Salkeld MSE, Kirk E. Smith BS, Bruce Whiting PhD, Robert L. Barrack MD**

Published online: 15 September 2009


**Abstract** Computed tomography (CT) may more accurately assess the healing of grafted osteolytic lesions around acetabular components compared with plain radiographs, although clinical validation is lacking. To determine whether clinical or micro-CT imaging could assess accurately the grafted lesion compared with histology, we therefore quantified bone healing and ingrowth to determine an effective rhBMP-2 dose and ratio to allograft bone when grafted adjacent to a cementless porous-coated component. We grafted surgically created acetabular defects in canines (n = 20) before uncemented total hip arthroplasty. At 6 weeks, embedded acetabula were imaged and the CT slice images matched to histology section images. The percentage of bone in the defect and growth into the porous surface was assessed quantitatively. Low-dose rhBMP-2 with allograft (1:5 ratio) resulted in a higher percentage of defect healing (43.8%) than rhBMP-2 alone (29.2%) and a higher percentage of bone ingrowth (15.7%) than allograft bone alone (1.1%) as measured by histology. Micro-CT measurements were similar to histologic measurements of defect healing, whereas clinical CT overestimated periprosthetic bone by 38%. Neither clinical CT nor micro-CT techniques are adequate for assessing ingrowth or the bone-implant interface with metal artifacts.

The institution of the authors (SDC, LPP, SLS) has received funding from Medtronic.
Each author certifies that his institution has approved the human and animal use protocols for this investigation, that all investigations were conducted in conformity with ethical principles of research, and that informed consent for clinical participation in the study was obtained. This work was performed at Washington University School of Medicine, Barnes-Jewish Hospital, St Louis, MO, and Fellowship of Orthopaedic Researchers, Metairie, LA.

S. D. Cook, L. P. Patron, S. L. Salkeld
Fellowship of Orthopaedic Researchers, Metairie, LA, USA

K. E. Smith, B. Whiting
Mallinckrodt Institute of Radiology, Washington University School of Medicine, St Louis, MO, USA

R. L. Barrack (✉)
Charles F. and Joanne Knight Distinguished Professor of Orthopaedic Surgery, Washington University School of Medicine, Barnes-Jewish Hospital, St Louis, MO 63110, USA
e-mail: barrackr@wustl.edu; pouchera@wustl.edu

## Introduction

During the 1990s, wear-related osteolysis emerged as a major issue in THA with an incidence ranging from 10% to 70% at 7 to 14 years depending on the implant type [10, 14, 17, 24, 28, 40, 41, 45]. Although the initial surgical approach to extensive acetabular osteolysis frequently involved component revision [21, 24, 26, 27, 34, 37, 47], acetabular shell retention with grafting of the lytic lesion subsequently became an increasingly popular option [24, 31, 34, 44]. Success of this approach required a mechanically stable, ingrown shell with an osteolytic lesion that did not involve the majority of the weightbearing area of the component [31]. Early detection of the presence, extent, and progression of osteolysis, therefore, became an important goal in clinical followup of these patients. Although periprosthetic osteolysis was initially identified and assessed with plain radiographs, CT techniques were quickly established as far more accurate in quantifying the presence and extent of these lesions [6, 13, 22, 23, 35, 46].

Cancellous allograft was used most commonly for bone defects adjacent to hip implants [3, 24–27, 31, 37, 44] and has observed a high degree of success based on clinical and radiographic results [5, 20, 30, 32, 33]. Increased interest in

the use of bone graft substitutes, including synthetics, demineralized bone matrix, and bone morphogenic protein (BMP) [1, 4, 7], has led to alternative grafting options with a need to objectively assess their healing adjacent to hip components. Both rhBMP-2 delivered with a calcium phosphate carrier and rhBMP-7 (OP-1) induced defect filling and bone ingrowth into porous acetabular components in a canine THA model [2, 4]. The use of these osteogenic agents, in combination with other graft materials and at reduced protein amounts, may compromise their ability to stimulate healing of periprosthetic defects in the hip and improve fixation and warrants further investigation.

Clinical studies have judged healing of periprosthetic lytic lesions mainly based on implant survival without revision and the appearance of the lesion on plain radiographs. CT imaging has been well established as a superior modality to plain radiography in assessing periprosthetic lytic lesions; however, there are limited data on CT assessment of healing in grafted lesions. In one study, a high percentage of lesions grafted with morsellized allograft were judged to have healed based on arbitrary CT criteria [35]; however, their success criteria were not validated using a gold standard such as histology. Given the time, cost, and morbidity associated with grafting these lesions, confirmation of the fate of the graft material is necessary to objectively judge this intervention's usefulness.

We designed the current study to investigate the ability of rhBMP-2 delivered on an absorbable collagen sponge (ACS) to induce bone healing and bone ingrowth into porous acetabular components using a canine THA model and specifically to (1) determine an effective volume ratio of rhBMP-2/ACS combined with allograft compared with the rhBMP-2 or allograft alone to induce bone healing and ingrowth; (2) determine whether a lower concentration or amount of protein would be as effective as a standard canine dose in the healing of this defect; and (3) assess whether clinical CT and micro-CT imaging techniques could be used to accurately quantify the bone healing and ingrowth compared with definitive histologic and microradiographic measurements.

## Materials and Methods

Institutional approval was obtained for all procedures and animal care performed in this study. The 20 adult mongrel dogs used in this study were randomized into five graft treatment groups with four dogs per group. Using surgical techniques previously described [2], the acetabulum was first prepared using sequential reamers to fit a 27-mm diameter component. We created a defect measuring 2 cm $\times$ 1 cm $\times$ 0.5 cm centrally in the dome of the acetabulum and grafted with 1 $cm^3$ of graft material: (1) allograft bone; (2) bone morphogenetic protein (BMP = rhBMP-2/ACS; Medtronic, Memphis, TN) alone; or (3) one of two ratios of rhBMP-2 to allograft with varying rhBMP-2 concentrations and protein amounts (Table 1). The technique for grafting included morsellization of the ACS, which was soaked with the rhBMP-2 solution for a minimum of 15 minutes and then mixed with the allograft in appropriate volumes (ratios) before implantation. The graft was placed into the acetabular defect immediately before impaction of the acetabular component, which had three metal spikes for additional stability. Unilateral THA was performed with a cementless, porous-coated titanium acetabular component and a canine femoral system (BioMedtrix, Allendale, NJ) similarly used in our previous study [2]. Based on previously published data examining the effects of BMP-7 on bone induction in the same canine model [2], the sample size to detect an 80% increase in defect healing (area fraction of bone) with a BMP-2-based graft compared with allograft bone was four ($\sigma = 7.5$; $\alpha = .05$; power = 80%).

Using standard aseptic techniques, surgery was performed under isoflurane gas anesthesia (induction up to 5%; maintenance 1%–5%) after preanesthesia induction with glycopyrrolate (0.01 mg/kg) and tiletamine/xylazine (1 mL/50 lb). Intravenous fluid support was maintained during the surgical procedures. Buprenorphine (0.01 mg/kg) was administered before surgery and postoperatively as required for pain management. Animals were administered intramuscular broad-spectrum antibiotics (penicillin G benzathine and procaine solution; 1 mL/20 lb) for 4 days after surgery. Animals were kept in recovery cages for 36 to 48 hours to restrict motion. After weightbearing was

**Table 1.** Summary of the five graft treatment groups

| Acetabular defect graft treatment groups | | Allograft volume | BMP concentration | BMP amount (mg) | BMP/ACS volume |
|---|---|---|---|---|---|
| 1 | Allograft bone | 1 cc | 0 | 0 | 0 |
| 2 | 1:5 BMP:allograft bone | 0.8 cc | 0.15 mg/mL | 0.030 mg | 0.2 cc |
| 3 | 1:5 BMP:allograft bone | 0.8 cc | 0.43 mg/mL | 0.086 mg | 0.2 cc |
| 4 | 1:1 BMP:allograft bone | 0.5 cc | 0.43 mg/mL | 0.215 mg | 0.5 cc |
| 5 | BMP | 0 | 0.43 mg/mL | 0.430 mg | 1 cc |

BMP = rhBMP-2/ACS (INFUSE ™ Bone Graft; Medtronic, Memphis, TN); ACS = absorbable collagen sponge.

demonstrated, the animals were allowed unrestricted motion in their runs. Clinical monitoring of the surgical sites and overall animal health was maintained during the study course. At the end of the 6-week study period, all animals were euthanized with an intravenous barbiturate overdose (Beuthanasia-D solution, 0.22 mL/kg). All components remained well-fixed and stable with no evidence of gross or radiographic loosening at 6 weeks. Pelvic and peri-implant tissues were removed and processed for imaging and histologic analysis.

Methyl methacrylate-embedded tissues were cored into 3-cm diameter cylindrical blocks centered about the 2.7-cm diameter acetabular component. The cored blocks were imaged using clinical and micro-CT scanning protocols. Clinical scans were obtained with a Sensation 64 scanner (Siemens Medical Solutions, Forchheim, Germany) using a dehiscence protocol with the following parameters: 120 kVp, 400 mAs effective, 1-second rotation time, and 0.6-mm collimation. The scans were obtained in spiral mode with 0.2 pitch, U70u kernel, 51-mm field of view, reconstruction interval of 0.1 mm, and 0.1-mm isotropic voxel. The micro-CT imaging was conducted with a SCANCO μCT 40 (SCANCO Medical AG, Basserdorf, Switzerland) set in standard mode: 70-kVp tube potential, 114-μA tube current, 200-ms integration time, and 36-μm isotropic voxel.

To facilitate comparison of CT, microradiograph, and histologic images, a reference coordinate system was established and notches were machined into each cylindrical core along the designated x and y axes. This coordinate system was used during thin sectioning, which allowed the location of each histologic section to be approximated within a respective CT volume. A landmark-based registration algorithm was used with the Analyze software (Biomedical Imaging Resource; Mayo Clinic, Rochester, MN) [36] to further align the clinical and micro-CT images with the microradiograph images of the histologic sections. The CT volumes were then transformed using the resulting registration matrix, and the corresponding image slice was extracted as a 16-bit uncompressed grayscale image for further analysis.

After CT imaging, the acetabula/components were sectioned (0.75 to 1 mm thickness) using a diamond blade on a high-speed water-cooled sectioning saw (Mark V, East Granby, CT). The coordinate reference markings on the block were used to orient the sectioning plane with that of the imaging slices. Four sections selected from each hip were bonded to acrylic slides and ground using a metallurgical grinder-polisher (Buehler, Lake Bluff, IL). These sections were further ground to 50 to 100 μm thickness, polished, and then stained with basic fuchsin and toluidine blue. Histology sections were imaged using a digital camera (DXM-1200; Nikon Instruments, Melville, NY) attached to a Nikon Eclipse E600 polarizing microscope (Nikon Instruments). Microradiographs of the finished sections (resolution 13.25 μm) were made using an X-ray cabinet (Faxitron X-Ray, Wheeling, IL) and high-resolution film (M-100; Eastman Kodak, Rochester, NY).

Quantitative measurements of the percentage of bone within the entire defect were performed on all histology sections using Image-Pro Plus software (Media Cybernetics, Silver Spring, MD). An area of interest (AOI) equivalent to the original defect was analyzed in the region surrounding the dome of the acetabular component. The percentage of ingrowth was measured within the 1-mm thickness area of the beaded coating (mean pore size of approximately 200 μm) spanning the defect area.

For the comparison of histology, clinical CT, and micro-CT images, bone area measurements were performed within a 4-mm × 4-mm AOI placed in the defect region. The AOI was uniformly applied to each section image within the defect and tangent to the dome surface. Spatial calibration settings used in the image assessments were: clinical CT (9.98 pixels/mm), micro-CT (27.7 pixels/mm), and microradiograph (75.3 pixels/mm) resulting from resolution differences. Optimal gray scale histogram ranges were used to select only regions of mineralized bone. The analysis was performed on 42 matched CT and microradiograph images with a minimum of two sections chosen from each of 20 hips.

In addition, the defect–implant interface was examined qualitatively for the degree of bone contact along the beaded surface of the component by assessing the histologic sections and microradiograph images of at least two sections from each hip. The presence of artifact was noted for both clinical CT and micro-CT imaging techniques.

We used analysis of variance to determine the differences in defect healing and bone ingrowth among the group means based on graft treatment. Paired t-test was used to compare the paired microradiograph and CT bone percentages measured in the AOI. The differences between the percent bone measured in each CT and matched microradiograph image were calculated and a 95% confidence interval was determined (BMDP Statistical Software, Inc, Los Angeles, CA).

## Results

The rhBMP-2 alone elicited de novo bone healing (29.2%) with minimal bone ingrowth (4.3%) and limited bone–implant contact (< 5%) at 6 weeks postimplantation using histologic sections as the gold standard. Allograft bone alone resulted in de novo bone formation (43.8%) with negligible bone ingrowth (1.1%) and a lack of bone–implant contact (0–5%). Any combination of rhBMP-2 and

allograft bone was better than rhBMP-2 alone in eliciting higher degrees ($p < 0.01$) of defect healing (43.4% versus 29.2%). Only the low-dose combination of rhBMP-2 and allograft (1:5, 0.03 mg) achieved a higher degree of defect healing than allograft bone alone. Any treatment involving rhBMP-2 led to a higher percent ($p = 0.04$) bone ingrowth and larger degree of bone–implant contact (range, 6%–75%) than allograft alone. The most effective combination in terms of bone ingrowth was combining rhBMP-2 with allograft, which outperformed both rhBMP-2 alone (12.4% versus 4.3%) and allograft bone alone (12.3% versus 1.1%) (Table 2).

The use of a lower concentration (0.15 mg/mL) and smaller amount (0.03 mg) of rhBMP-2 combined with allograft at a ratio of 1:5 achieved a higher percentage ($p = 0.01$) of defect healing than rhBMP-2 alone (48.4% versus 29.2%), which was administered at the standard canine dose concentration (0.43 mg/mL). The low-dose rhBMP-2 (0.03 mg) with allograft also had a higher percentage ($p < 0.01$) of bone ingrowth than allograft bone alone (15.7% versus 1.1%) as measured by histology (Table 2).

Regardless of graft treatment, the percent bone measured in the micro-CT images (mean 33.6%, 95% CI = 28.3%–39.0%) was similar ($p = 0.93$) to that measured in the matched histology images (mean 33.7%, 95% CI = 29.5%–38.0%) (Table 3). The regression of micro-CT to histology percent bone showed a strong linear correlation ($R^2 = 0.7$, $y = 1.00x$) (Fig. 1). The clinical CT measurements (mean 46.5%, 95% CI = 38.1%–54.8%) were 12.8% higher on average compared with histologic measurements (Table 3), which corresponds to an overestimation ($p < 0.001$) of the degree of bone healing in the defect averaging 38% (12.8/33.7) (Fig. 2).

With neither clinical CT nor micro-CT were we able to assess the interface between bone and the surface of the implant as a result of the blurring, voids, and streaking

**Table 2.** Comparison of histologic defect healing and bone ingrowth of the entire defect and defect–implant interface among five graft treatment groups (mean ± SD)

| Graft treatment | Percent bone defect healing | Bone ingrowth |
|---|---|---|
| Allograft bone | 43.8% ± 4.8% | 1.1% ± 1.9% |
| 1:5 BMP:allograft (0.03 mg) | 48.4% ± 9.2% | 15.7% ± 7.5% |
| 1:5 BMP:allograft (0.09 mg) | 40.9% ± 5.6% | 8.9% ± 1.5% |
| 1:1 BMP:allograft (0.22 mg) | 40.9% ± 7.0% | 12.4% ± 11.3% |
| BMP (0.43 mg) | 29.2% ± 6.0% | 4.3% ± 3.8% |
| Analysis of variance p value | 0.014 BMP versus allograft, BMP versus 1:5 ratio (0.03 mg) | 0.036 allograft versus all other groups |

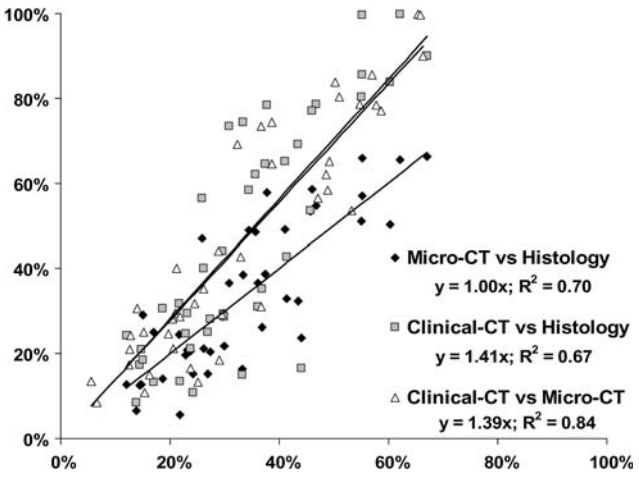


**Fig. 1** Correlation of clinical CT and micro-CT measurements to quantitative histology is shown in this graph. We observed a strong positive correlation ($r = 0.82$–$0.84$) between the CT and histology measurements of bone. The clinical CT measurements of bone were increased relative to histology and micro-CT measurements as evidenced by the shifted slopes (39%–41%).

**Table 3.** Bone area measurements of representative areas of interest comparing histologic sections, micro-CT, and clinical CT images by graft treatment and pooled (mean bone % [95% confidence limits])

| Graft treatment | Histology (bone %) | Micro-CT (bone %) | Clinical CT (bone %) |
|---|---|---|---|
| Allograft bone | 32.9 (27.4–38.4) | 35.6 (29.1–42.2) | 50.4 (40.1–60.7) |
| 1:5 BMP:allograft (0.03 mg) | 37.3 (33.8–40.7) | 35.9 (30.7–41.1) | 43.4 (36.1–50.8) |
| 1:5 BMP:allograft (0.09 mg) | 40.0 (35.0–45.1) | 39.2 (33.9–44.5) | 53.1 (43.9–62.2) |
| 1:1 BMP:allograft (0.22 mg) | 32.5 (28.7–36.3) | 33.8 (29.1–38.5) | 51.6 (43.3–59.8) |
| BMP (0.43 mg) | 25.4 (22.8–27.9) | 22.9 (18.2–27.6) | 32.3 (25.9–38.7) |
| Pooled; all treatment groups | 33.7 (29.5–38.0) | 33.6 (28.3–39.0) | 46.5 (38.1–54.8) |
| Paired t-test, two-tailed | $p = 0.93$, micro-CT versus histology | | |
| | $p < 0.001$, clinical CT versus histology | | |
| | $p < 0.001$, clinical CT versus micro-CT | | |

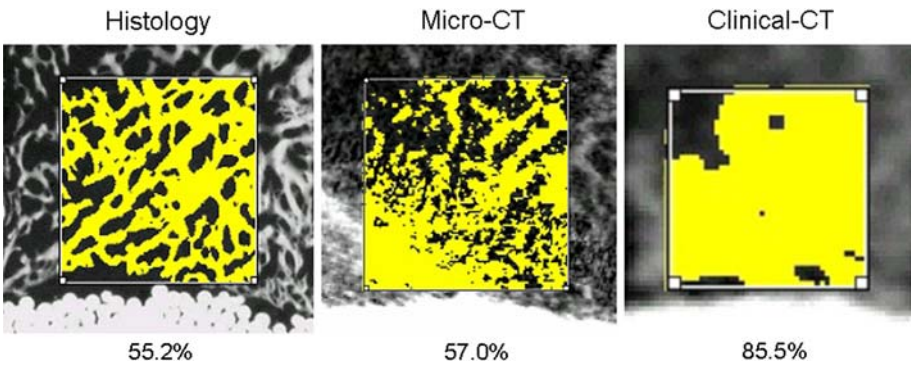


**Fig. 2** Histology correlated closely with micro-CT measurements, whereas clinical CT measurements showed higher levels of bone fill than histology resulting from lower resolution.

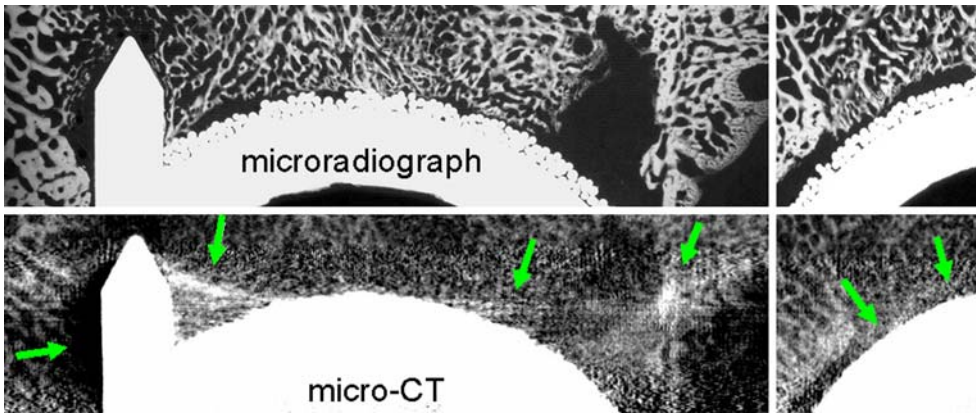


**Fig. 3** Metal artifact of micro-CT compared with microradiograph prevented assessment of bone ingrowth and caused distortion close to the metal surface despite application of all available postprocessing metal artifact manipulations.

attributed to metal artifacts (Fig. 3). These effects made it impossible to assess the percentage of bone apposition or ingrowth to the porous surface.

## Discussion

In recent years, numerous authors have concluded that spiral CT is more accurate than plain radiographs in assessing lytic lesions adjacent to total hip components [6, 22, 23, 42], and, based on such findings, periodic CT scanning for surveillance of lytic lesions after cementless THA has been recommended [43]. Studies have generally relied on the radiographic appearance of grafted lytic lesions such that the actual fate of the lesions is unproven [18, 39]. Although studies have emphasized the accuracy of CT in assessing lesion volume, far less data are available on its ability to quantify the healing of grafted lesions adjacent to cementless components [11, 35]. Yet in the clinical scenario, CT measurements of grafted lesions remain unconfirmed absent biopsy at subsequent reoperation or postmortem retrieval, both of which occur too sporadically to rely on for validation. Therefore, there remains a need to validate the efficacy of materials used to graft lytic lesions as well as a need to assess with some clinical accuracy their degree of success to justify their use.

Using a previously described and validated canine model [2], this study investigated effective graft options, including volume ratio and dose concentration, of a recombinant rhBMP-2 combined with allograft bone for the induction of healing in an acetabular bone defect and ingrowth into an adjacent noncemented porous component. The measurements of the extent of healing and ingrowth using histology and microradiography served to validate whether clinical CT and micro-CT imaging techniques were accurate in quantifying the same healing parameters.

Our study has several limitations. First, we used only one early time point of healing (6 weeks). Bone induction by BMP-2 occurs rapidly in canine defect healing models; therefore, the early time point was chosen to capture the rapid bone-induced healing with a BMP graft and to detect potential differences in healing based on graft ratios and dose. The addition of later time points would allow for a determination of the healing progression and maturity of bone over time. Second, there were no empty defects or defects treated with autogenous bone graft studied in this experiment. Although an empty defect was used in a previous study to evaluate OP-1 on healing in the same model [2], it would have added limited value to this short-term healing study to evaluate effective grafting options with BMP-2. Similarly, autograft was not used as a graft option in the current study because cancellous allograft bone is an

accepted standard for such grafting. Third is the inherent limits of an animal study as it relates to the clinical condition; animals, and dogs in particular, generally remodel at faster rates than humans. Fourth, the assessment methods of this study may not be relevant to periprosthetic defects in other locations or necessarily in humans; however, the findings do provide valuable information on the usefulness and limitations of CT imaging techniques in the accurate assessment of grafted defects in the hip.

Although any combination of rhBMP-2 and allograft bone elicited a higher degree of healing than the rhBMP-2 alone (43.4% versus 29.2%) and substantially greater ingrowth than allograft alone (12.3% versus 1.1%), the 1:5 volume ratio of rhBMP-2 to allograft was the most effective in achieving the highest percentage of defect healing, bone ingrowth, and apposition. The overall efficacy of the 1:5 volume ratio of rhBMP-2/ACS to allograft was not decreased compared with that of the 1:1 volume ratio in this acetabular defect model of healing. Another study by Jones et al. suggests that extending rhBMP-2/ACS past a 1:1 volume ratio to cancellous allograft or a ceramic may limit its efficacy as demonstrated in a canine critical-sized segmental defect model [16]. In a canine THA model, Bragdon et al. demonstrated improved porous ingrowth (23%) and local bone promotion of defect healing with an unreported ratio of rhBMP-2 and a calcium phosphate carrier (α-BSM) [4]. Their 0.4 mg rhBMP-2 dose per acetabular defect is similar to the 0.43 mg rhBMP-2 dose delivered without additional graft used in our study. In a similar canine model, BMP-7 (0.77 mg rhOP-1) achieved substantially greater defect healing (37% versus 23%) and bone ingrowth (37% versus 19%) compared with allograft bone alone, although combinations of BMP-7 and allograft and other doses were not evaluated [2].

Histologic and microradiographic results of the current study indicated that among the graft preparations used, the lowest concentration of BMP (0.03 mg rhBMP-2) was associated with the highest percentage of defect healing and bone ingrowth into the porous surface, whereas BMP alone (0.43 mg rhBMP-2) had the lowest percent bone defect healing (29.2%) and allograft bone had the lowest percentage bone ingrowth (1.1%). The explanation for lower doses of rhBMP-2 resulting in higher percentages of bone healing is unclear. Numerous studies show that carriers dramatically affect the efficacy of BMPs [9, 12, 15]. In addition, BMPs are known to accelerate the rate of bone resorption as well as bone formation [19, 29, 38] so that lower doses when combined with osteoconductive carriers or grafts may result in equivalent or superior efficacy compared with higher doses.

Our data show that micro-CT correlates with histology in quantifying defect healing, whereas clinical CT overestimates the degree of healing by 38%. The micro-CT findings were consistent with those of Cowan et al., who found micro-CT was highly accurate in assessing the quality and quantity of defect healing with bone protein in a rat calvarial model [8]. In their study, micro-CT delineated some ultrastructural details of graft incorporation not possible with the histologic technique used, yet a considerable benefit was that the resolution of their micro-CT data was not adversely affected by any artifacts as a result of the presence of metal. The lower resolution of clinical CT undoubtedly contributed to the lower correlation with histology in this study. Current-generation micro-CT has a resolution more than three times higher than clinical CT (approximately 36 μm versus 100 μm) but is restricted to relatively small specimens and requires a much higher radiation dose. The CT was particularly inaccurate in the area adjacent to the porous surface as a result of the presence of artifact [7]. Despite numerous postreconstruction processing strategies such as the use of extended Hounsfield unit scaling and the application of smoothing filters, the effects of metal artifact prevented an accurate assessment of bone–implant apposition or ingrowth to the porous surface using either CT imaging technique. Perhaps with technology advancements of the scanners and using metal-artifact reduction schemes during scanning, the accuracy of clinical CT scans may be improved.

Our data indicate the combination of smaller amounts of rhBMP-2 with allograft bone was more effective than the rhBMP-2 or allograft alone in inducing acetabular bone defect healing and porous ingrowth in a canine THA model. Micro-CT is an effective surrogate for histology and microradiographs for quantifying healing of these bone defects and is accurate enough to distinguish fairly small differences in efficacy among different graft materials. Clinical CT consistently overestimates graft incorporation and defect healing and is not accurate enough to distinguish small differences in healing among different graft materials. Neither clinical nor micro-CT can evaluate the bone–implant interface to quantify osseointegration or bone ingrowth with the current state of imaging technology.

## References

1. Barrack RL. Bone graft extenders, substitutes, and osteogenic proteins. *J Arthroplasty.* 2005;20(Suppl 2):94–97.
2. Barrack RL, Cook SD, Patron LP, Salkeld SL, Szuszczewicz E, Whitecloud TS 3rd. Induction of bone ingrowth from acetabular defects to a porous surface with OP-1. *Clin Orthop Relat Res.* 2003;417:41–49.
3. Benson ER, Christensen CP, Monesmith EA, Gomes SL, Bierbaum BE. Particulate bone grafting of osteolytic femoral lesions around stable cementless stems. *Clin Orthop Relat Res.* 2000;381:58–67.
4. Bragdon CR, Doherty AM, Rubash HE, Jasty M, Li XJ, Seeherman H, Harris WH. The efficacy of BMP-2 to induce bone

ingrowth in a total hip replacement model. *Clin Orthop Relat Res.* 2003;417:50–61.
5. Buma P, Donk S, Slooff TJ, Schreurs W. Bone graft incorporation after reconstruction of bony defects with impacted morselized bone graft. Histology of animals and patients. *Orthop Traumatol Rehabil.* 2001;3:41–47.
6. Claus AM, Totterman SM, Sychterz CJ, Tamez-Pena JG, Looney RJ, Engh CA, Sr. Computed tomography to assess pelvic lysis after total hip replacement. *Clin Orthop Relat Res.* 2004;422: 167–174.
7. Cook SD, Salkeld SL, Patron LP, Barrack RL. The effect of demineralized bone matrix gel on bone ingrowth and fixation of porous implants. *J Arthroplasty.* 2002;17:402–408.
8. Cowan CM, Aghaloo T, Chou YF, Walder B, Zhang X, Soo C, Ting K, Wu B. MicroCT evaluation of three-dimensional mineralization in response to BMP-2 doses in vitro and in critical sized rat calvarial defects. *Tissue Eng.* 2007;13:501–512.
9. Degat MC, Dubreucq G, Meunier A, Dahri-Correia L, Sedel L, Petite H, Logeart-Avramoglou D. Enhancement of the biological activity of BMP-2 by synthetic dextran derivatives. *J Biomed Mater Res A.* 2009;88:174–183.
10. Dumbleton JH, Manley MT, Edidin AA. A literature review of the association between wear rate and osteolysis in total hip arthroplasty. *J Arthroplasty.* 2002;17:649–661.
11. Engh CA Jr, Egawa H, Beykirch SE, Hopper RH Jr, Engh CA. The quality of osteolysis grafting with cementless acetabular component retention. *Clin Orthop Relat Res.* 2007;465:150–154.
12. Fu YC, Nie H, Ho ML, Wang CK, Wang CH. Optimized bone regeneration based on sustained release from three-dimensional fibrous PLGA/HAp composite scaffolds loaded with BMP-2. *Biotechnol Bioeng.* 2008;99:996–1006.
13. Garcia-Cimbrelo E, Tapia M, Martin-Hervas C. Multislice computed tomography for evaluating acetabular defects in revision THA. *Clin Orthop Relat Res.* 2007;463:138–143.
14. Glyn-Jones S, Isaac S, Hauptfleisch J, McLardy-Smith P, Murray DW, Gill HS. Does highly cross-linked polyethylene wear less than conventional polyethylene in total hip arthroplasty? A double-blind, randomized, and controlled trial using roentgen stereophotogrammetric analysis. *J Arthroplasty.* 2008;23: 337–343.
15. Jeon O, Song SJ, Yang HS, Bhang SH, Kang SW, Sung MA, Lee JH, Kim BS. Long-term delivery enhances in vivo osteogenic efficacy of bone morphogenetic protein-2 compared to short-term delivery. *Biochem Biophys Res Commun.* 2008;369:774–780.
16. Jones CB, Sabatino CT, Badura JM, Sietsema DL, Marotta JS. Improved healing efficacy in canine ulnar segmental defects with increasing recombinant human bone morphogenetic protein-2/ allograft ratios. *J Orthop Trauma.* 2008;22:550–559.
17. Kawamura H, Dunbar MJ, Murray P, Bourne RB, Rorabeck CH. The porous coated anatomic total hip replacement. A ten to fourteen-year follow-up study of a cementless total hip arthroplasty. *J Bone Joint Surg Am.* 2001;83:1333–1338.
18. Kelly MP, Kitamura N, Leung SB, Engh CA Sr. The natural history of osteoarthritic bone cysts after uncemented total hip arthroplasty. *J Arthroplasty.* 2007;22:1137–1142.
19. Lane JM. Bone morphogenic protein science and studies. *J Orthop Trauma.* 2005;19(Suppl):S17–S22.
20. Leopold SS, Jacobs JJ, Rosenberg AG. Cancellous allograft in revision total hip arthroplasty. A clinical review. *Clin Orthop Relat Res.* 2000;371:86–97.
21. Leopold SS, Rosenberg AG, Bhatt RD, Sheinkop MB, Quigley LR, Galante JO. Cementless acetabular revision. Evaluation at an average of 10.5 years. *Clin Orthop Relat Res.* 1999;369:179–186.
22. Leung S, Naudie D, Kitamura N, Walde T, Engh CA. Computed tomography in the assessment of periacetabular osteolysis. *J Bone Joint Surg Am.* 2005;87:592–597.
23. Malchau H, Potter HG. How are wear-related problems diagnosed and what forms of surveillance are necessary? *J Am Acad Orthop Surg.* 2008;16(Suppl 1):S14–S19.
24. Maloney W, Rosenberg A. What is the outcome of treatment for osteolysis? *J Am Acad Orthop Surg.* 2008;16(Suppl 1):S26–S32.
25. Maloney WJ. The surgical management of femoral osteolysis. *J Arthroplasty.* 2005;20(Suppl 2):75–78.
26. Maloney WJ, Herzwurm P, Paprosky W, Rubash HE, Engh CA. Treatment of pelvic osteolysis associated with a stable acetabular component inserted without cement as part of a total hip replacement. *J Bone Joint Surg Am.* 1997;79:1628–1634.
27. Maloney WJ, Paprosky W, Engh CA, Rubash H. Surgical treatment of pelvic osteolysis. *Clin Orthop Relat Res.* 2001;393: 78–84.
28. Marshall A, Ries MD, Paprosky W. How prevalent are implant wear and osteolysis, and how has the scope of osteolysis changed since 2000? *J Am Acad Orthop Surg.* 2008;16(Suppl 1):S1–S6.
29. Mont MA, Ragland PS, Biggins B, Friedlaender G, Patel T, Cook S, Etienne G, Shimmin A, Kildey R, Rueger DC, Einhorn TA. Use of bone morphogenetic proteins for musculoskeletal applications An overview. *J Bone Joint Surg Am.* 2004;86(Suppl 2):41–55.
30. Mullaji AB, Marawar SV. Primary total hip arthroplasty in protrusio acetabuli using impacted morsellized bone grafting and cementless cups: a medium-term radiographic review. *J Arthroplasty.* 2007;22:1143–1149.
31. O'Brien JJ, Burnett RS, McCalden RW, MacDonald SJ, Bourne RB, Rorabeck CH. Isolated liner exchange in revision total hip arthroplasty: clinical results using the direct lateral surgical approach. *J Arthroplasty.* 2004;19:414–423.
32. Oakes DA, Cabanela ME. Impaction bone grafting for revision hip arthroplasty: biology and clinical applications. *J Am Acad Orthop Surg.* 2006;14:620–628.
33. Ogawa H, Ito Y, Itokazu M, Mori N, Shimizu T, Terabayashi N, Ishimaru D, Shimizu K. Morcellized bone grafting for acetabular deficiency in cementless total hip arthroplasty. *Orthopedics.* 2008;31:986.
34. Paprosky WG, Lawrence JM, Cameron HU. Classification and treatment of the failed acetabulum: a systematic approach. *Contemp Orthop.* 1991;22:121–130.
35. Puri L, Lapinski B, Wixson RL, Lynch J, Hendrix R, Stulberg SD. Computed tomographic follow-up evaluation of operative intervention for periacetabular lysis. *J Arthroplasty.* 2006; 21(Suppl 2):78–82.
36. Robb RA. The biomedical imaging resource at Mayo Clinic. *IEEE Trans Med Imaging.* 2001;20:854–867.
37. Rubash HE, Sinha RK, Maloney WJ, Paprosky WG. Osteolysis: surgical treatment. *Instr Course Lect.* 1998;47:321–329.
38. Sandhu HS, Khan SN. Animal models for preclinical assessment of bone morphogenetic proteins in the spine. *Spine.* 2002; 27(Suppl 1):S32–S38.
39. Schmalzried TP, Fowble VA, Amstutz HC. The fate of pelvic osteolysis after reoperation. No recurrence with lesional treatment. *Clin Orthop Relat Res.* 1998;350:128–137.
40. Schmalzried TP, Jasty M, Harris WH. Periprosthetic bone loss in total hip arthroplasty. Polyethylene wear debris and the concept of the effective joint space. *J Bone Joint Surg Am.* 1992;74: 849–863.
41. Soto MO, Rodriguez JA, Ranawat CS. Clinical and radiographic evaluation of the Harris-Galante cup: incidence of wear and osteolysis at 7 to 9 years follow-up. *J Arthroplasty.* 2000;15: 139–145.
42. Stamenkov R, Howie D, Taylor J, Findlay D, McGee M, Kourlis G, Carbone A, Burwell M. Measurement of bone defects adjacent to acetabular components of hip replacement. *Clin Orthop Relat Res.* 2003;412:117–124.

43. Stulberg SD, Wixson RL, Adams AD, Hendrix RW, Bernfield JB. Monitoring pelvic osteolysis following total hip replacement surgery: an algorithm for surveillance. *J Bone Joint Surg Am.* 2002;84(Suppl 2):116–122.
44. Terefenko KM, Sychterz CJ, Orishimo K, Engh CA Sr. Polyethylene liner exchange for excessive wear and osteolysis. *J Arthroplasty.* 2002;17:798–804.
45. Udomkiat P, Dorr LD, Wan Z. Cementless hemispheric porous-coated sockets implanted with press-fit technique without screws: average ten-year follow-up. *J Bone Joint Surg Am.* 2002;84: 1195–1200.
46. Walde TA, Weiland DE, Leung SB, Kitamura N, Sychterz CJ, Engh CA Jr, Claus AM, Potter HG, Engh CA Sr. Comparison of CT, MRI, and radiographs in assessing pelvic osteolysis: a cadaveric study. *Clin Orthop Relat Res.* 2005;437:138–144.
47. Weeden SH, Paprosky WG. Porous-ingrowth revision acetabular implants secured with peripheral screws. A minimum twelve-year follow-up. *J Bone Joint Surg Am.* 2006;88:1266–1271.